Chemical Engineering Science 63 (2008) 4531 – 4542

Contents lists available at ScienceDirect

Chemical Engineering Science

journal homepage: www.elsevier.com/locate/ces

Dynamic output feedback covariance control of stochastic dissipative partial differential equations

Gangshi Hu[b], Yiming Lou[a], Panagiotis D. Christofides[b,c,*]

[a]Advanced Projects Research, Inc., 1925 McKinley Avenue, Suite B, La Verne, CA 91750, USA
[b]Department of Chemical and Biomolecular Engineering, University of California, Los Angeles, CA 90095, USA
[c]Department of Electrical Engineering, University of California, Los Angeles, CA 90095, USA

ARTICLE INFO

Article history:
Received 5 December 2007
Received in revised form 19 June 2008
Accepted 30 June 2008
Available online 4 July 2008

Keywords:
Covariance control
Stochastic state estimation
Dynamic output feedback control
Stochastic PDEs
Surface roughness control

ABSTRACT

In this work, we develop a method for dynamic output feedback covariance control of the state covariance of linear dissipative stochastic partial differential equations (PDEs) using spatially distributed control actuation and sensing with noise. Such stochastic PDEs arise naturally in the modeling of surface height profile evolution in thin film growth and sputtering processes. We begin with the formulation of the stochastic PDE into a system of infinite stochastic ordinary differential equations (ODEs) by using modal decomposition. A finite-dimensional approximation is then obtained to capture the dominant mode contribution to the surface roughness profile (i.e., the covariance of the surface height profile). Subsequently, a state feedback controller and a Kalman–Bucy filter are designed on the basis of the finite-dimensional approximation. The dynamic output feedback covariance controller is subsequently obtained by combining the state feedback controller and the state estimator. The steady-state expected surface covariance under the dynamic output feedback controller is then estimated on the basis of the closed-loop finite-dimensional system. An analysis is performed to obtain a theoretical estimate of the expected surface covariance of the closed-loop infinite-dimensional system. Applications of the linear dynamic output feedback controller to both the linearized and the nonlinear stochastic Kuramoto–Sivashinsky equations (KSEs) are presented. Finally, nonlinear state feedback controller and nonlinear output feedback controller designs are also presented and applied to the nonlinear stochastic KSE.

1. Introduction

The recent efforts on feedback control and optimization of thin film growth processes to achieve desired material microstructure (see, for example, Choo et al., 2005; Christofides and Armaou, 2006; Christofides et al., 2008 and the references therein) have been motivated by the fact that the electrical and mechanical properties of thin films strongly depend on microstructural features such as interface width, island density and size distributions (Akiyama et al., 2002; Lee et al., 1999), which significantly affect device performance. To fabricate thin film devices with high and consistent performance, it is desirable that the operation of thin film growth processes is tightly controlled.

In terms of results on control of thin film surface microstructure, kinetic Monte-Carlo (kMC) models were initially used to develop a methodology for feedback control of thin film surface roughness (Lou and Christofides, 2003a,b). The method was successfully applied to control surface roughness in a gallium arsenide (GaAs) deposition process model (Lou and Christofides, 2004) and to control complex deposition processes including multiple components with both short-range and long-range interactions (Ni and Christofides, 2005a). Furthermore, a method for computationally efficient optimization of thin film growth using coupled macroscopic and microscopic models was developed (Varshey and Armaou, 2005). However, the fact that kMC models are not available in closed-form makes it very difficult to use them for system-level analysis and the design and implementation of model-based feedback control systems. To achieve better closed-loop performance, it is desirable to design feedback controllers on the basis of closed-form process models, which account for the stochastic nature of the microscopic events. An approach was reported in Siettos et al. (2003), Armaou et al. (2004) and Varshney and Armaou (2006) to identify linear deterministic models from outputs of kMC simulators and design controllers using linear control theory. This approach is effective in controlling macroscopic variables which are low statistical moments of the microscopic distributions (e.g., surface coverage, which is the first moment of species

* Corresponding author at: Department of Electrical Engineering, University of California, Los Angeles, CA 90095, USA. Tel.: +1 310 794 1015; fax: +1 310 206 4107.
E-mail addresses: ylou@ieee.org (Y. Lou), pdc@seas.ucla.edu (P.D. Christofides).

0009-2509/$ - see front matter © 2008 Elsevier Ltd. All rights reserved.
doi:10.1016/j.ces.2008.06.026

distribution on a lattice). However, to control higher statistical moments of the microscopic distributions, such as the surface roughness (the second moment of height distribution on a lattice) or even the microscopic configuration (such as the surface morphology), deterministic models may not be sufficient and stochastic partial differential equation (PDE) models may be needed. In this area, other results include the construction of reduced-order approximations of the master equation (Gallivan and Murray, 2004) and control of a coupled kMC and finite-difference simulation code of a copper electro-deposition process using empirical input–output models (Rusli et al., 2006).

Stochastic PDEs arise naturally in the modeling of surface morphology of ultra thin films in a variety of material preparation processes (Edwards and Wilkinson, 1982; Villain, 1991; Vvedensky et al., 1993; Cuerno et al., 1995; Lauritsen et al., 1996). For example, it has been experimentally verified that the Kardar–Parisi–Zhang (KPZ) equation (Kardar et al., 1986) can describe the evolution of the surface morphology of GaAs thin films (Ballestad et al., 2002; Kan et al., 2004). When a stochastic PDE is used to model the height of the surface in a thin film growth process, there is a clear physical meaning of the state covariance of the solution of the stochastic PDE, which is the expected surface roughness of the thin film. It was demonstrated that this link between the state covariance of the stochastic PDE model and the material microstructure can be used to design model-based feedback controllers for real-time regulation of material microstructure (Lou and Christofides, 2005a,b). This practical consideration has motivated recent efforts on covariance control of stochastic PDEs. Specifically, methods for state feedback covariance control for linear (Lou and Christofides, 2005a,b; Ni and Christofides, 2005b) and nonlinear (Lou and Christofides, 2006) stochastic PDEs have been developed. The methods involve the reformulation of a stochastic PDE into a system of infinite linear/nonlinear stochastic ordinary differential equations (ODEs) by using modal decomposition, derivation of a finite-dimensional approximation that captures the dominant mode contribution to the surface roughness, and state feedback controller design based on the finite-dimensional approximation. Modal decomposition is advantageous for model reduction of dissipative PDEs, because one of the characteristics of dissipative PDEs is the separation of the eigenspectrum of the spatial differential operator into fast and slow modes. Modal decomposition takes advantage of this characteristic of the system and results in a computationally efficient way to derive a low-order, finite-dimensional system that captures the dominant modal contribution to the surface roughness and can be used as a basis for feedback controller design. As a comparison, finite element methods (FEMs) are brute-force local discretization methods, which result in high-order finite-dimensional approximations and very high-order controllers that cannot be practically implemented in real-time control applications (Christofides, 2001).

Furthermore, although stochastic PDE models are suitable for model-based controller design, the construction of stochastic PDE models directly based on microscopic process rules is, in general, a very difficult task. This has motivated the development of system identification methods for stochastic PDEs. Compared to deterministic systems, modeling and identification of dynamical systems described by stochastic ordinary/partial differential equations has received relatively limited attention and most of the results focus on stochastic ODE systems using likelihood-based methods (Åström, 1970; Bohlin and Graebe, 1995; Kristensen et al., 2004). In our recent research, we found that the dynamics of the statistical moments of the state of a stochastic process may be described by a deterministic differential equation, and the issues of parameter estimation for stochastic models could be addressed by employing parameter estimation techniques for deterministic systems. Following this idea, methods for identification and construction of linear stochastic PDE models were developed (Lou and Christofides, 2005a; Ni and Christofides, 2005b). More recently, a method for construction of nonlinear stochastic PDEs was also developed (Hu et al., 2008). Using these methods, linear/nonlinear stochastic PDE models can be constructed from the kinetic Monte-Carlo simulation data of the microscopic process.

However, so far, only state feedback covariance controllers have been developed for stochastic PDEs. In the design of a state feedback controller, it is assumed that the full state of the PDE can be measured in real-time at all positions and times. This assumption is not practical in many applications, where process output measurements are typically available from a finite (usually small) number of measurement sensors. Therefore, there is a strong motivation to develop dynamic output feedback covariance control methods for stochastic PDEs, which couple a state feedback control law to a dynamic state observer that utilizes information from few measurement sensors. The observer-based covariance control structure for linear stochastic ODE systems was proposed in Hotz and Skelton (1987), Iwasaki and Skelton (1994), in which a Kalman filter is used as a state estimator and the estimated state is used by the feedback controller. However, the problem of output feedback covariance control for nonlinear systems and infinite-dimensional systems has not been studied.

In this work, a method is developed for dynamic output feedback covariance control of the state covariance of linear dissipative stochastic PDEs. Spatially distributed control actuation and sensor measurements with noise are considered when designing the dynamic output feedback controller. We initially formulate the stochastic PDE into a system of infinite stochastic ODEs by using modal decomposition and construct a finite-dimensional approximation to capture the dominant mode contribution to the surface covariance of the height profile. Subsequently, a state feedback controller and a Kalman–Bucy filter are designed on the basis of the finite-dimensional approximation. The dynamic output feedback controller is obtained by combining the state feedback controller and the state estimator. Analysis of the closed-loop stability and the steady-state surface covariance under the dynamic output feedback controller are provided for the finite-dimensional approximation and the infinite-dimensional system. Applications of the linear dynamic output feedback controller to both the linearized and the nonlinear stochastic Kuramoto–Sivashinsky equation (KSE) are presented. We also present nonlinear state feedback controller and nonlinear output feedback controller designs and apply them to the nonlinear stochastic KSE.

2. Preliminaries

2.1. Stochastic PDEs with distributed control

We focus on linear dissipative stochastic PDEs with distributed control of the following form:

$$\frac{\partial h}{\partial t} = \mathscr{A}h + \sum_{i=1}^{p} b_i(x)u_i(t) + \xi(x,t) \tag{1}$$

subject to homogeneous boundary conditions and the initial condition $h(x,0)=h_0(x)$, where $x \in [-\pi,\pi]$ is the spatial coordinate, t is the time, $h(x,t)$ is the state of the PDE which corresponds to the height of the surface in a thin film growth process at position x and time t, $\mathscr{A}$ is a dissipative, self-adjoint spatial differential operator, $u_i(t)$ is the ith manipulated input, p is the number of manipulated inputs and $b_i(x)$ is the ith actuator distribution function (i.e., $b_i(x)$ determines how the control action computed by the ith control actuator, $u_i(t)$, is distributed (e.g., point or distributed actuation) in the spatial interval $[-\pi,\pi]$). $\xi(x,t)$ is a Gaussian white noise with the following

expressions for its mean and covariance:

$$\langle \xi(x,t)\rangle = 0$$
$$\langle \xi(x,t)\xi(x',t')\rangle = \sigma^2\delta(x-x')\delta(t-t') \quad (2)$$

where σ is a real number, $\delta(\cdot)$ is the Dirac delta function and $\langle\cdot\rangle$ denotes the expected value. Gaussian white noise is chosen as the noise term in the stochastic PDE. The Gaussian white noise is a natural choice and works well in many process models. For example, stochastic PDEs with Gaussian white noise are reported in the modeling of surface height evolution of many microscopic processes, such as random deposition with surface relaxation, ballistic deposition and sputtering processes (Edwards and Wilkinson, 1982; Cuerno et al., 1995; Lauritsen et al., 1996).

Our objective is to control the surface covariance of the process, Cov_h, which is represented by the expected value of the standard deviation of the surface height from the desired height and is given as follows:

$$\mathrm{Cov}_h(t) = \left\langle \int_{-\pi}^{\pi} [h(x,t) - h_d]^2 \,\mathrm{d}x \right\rangle \quad (3)$$

where $h_d(t)$ is the desired surface height.

To study the dynamics of Eq. (1), we initially consider the eigenvalue problem of the linear spatial differential operator of Eq. (1) subject to the operator homogenous boundary conditions, which takes the form

$$\mathscr{A}\bar{\phi}_n(x) = \lambda_n\bar{\phi}_n(x), \quad n = 1,2,\ldots \quad (4)$$

where λ_n and $\bar{\phi}_n$ denote the nth eigenvalue and eigenfunction, respectively. To simplify our development and motivated by most practical applications, we consider stochastic PDEs for which $\mathscr{A}$ is a highly dissipative, self-adjoint operator (i.e., a second-order or fourth-order linear self-adjoint operator) and has eigenvalues which are real and satisfy $\lambda_1 \geqslant \lambda_2 \cdots$ and the sum $\sum_{i=1,\lambda_i\neq 0}^{\infty} |1/\lambda_i|$ converges to a finite positive number. Furthermore, the eigenfunctions $\{\bar{\phi}_1(x), \bar{\phi}_2(x), \ldots\}$ form a complete orthonormal set.

To present the method for feedback controller design, we initially formulate Eq. (1) into an infinite-dimensional stochastic ODE system using modal decomposition. To this end, we first expand the solution of Eq. (1) into an infinite series in terms of the eigenfunctions of the operator $\mathscr{A}$ as follows:

$$h(x,t) = \sum_{n=1}^{\infty} \alpha_n(t)\bar{\phi}_n(x) \quad (5)$$

where $\alpha_n(t)$ $(n = 1,2,\ldots,\infty)$ are time-varying coefficients. Substituting the above expansion for the solution, $h(x,t)$, into Eq. (1) and taking the inner product with $\bar{\phi}_n(x)$, the following system of infinite stochastic ODEs is obtained:

$$\frac{\mathrm{d}\alpha_n}{\mathrm{d}t} = \lambda_n\alpha_n + \sum_{i=1}^{p} b_i^n u_i(t) + \xi^n(t), \quad n = 1,\ldots,\infty \quad (6)$$

where

$$b_i^n = \int_{-\pi}^{\pi} \bar{\phi}_n(x) b_i(x)\,\mathrm{d}x \quad (7)$$

and

$$\xi^n(t) = \int_{-\pi}^{\pi} \xi(x,t)\bar{\phi}_n(x)\,\mathrm{d}x \quad (8)$$

The covariance of $\xi_\alpha^n(t)$ can be computed by using the following result:

Result 1. If (1) $f(x)$ is a deterministic function, (2) $\eta(x)$ is a random variable with $\langle\eta(x)\rangle = 0$ and covariance $\langle\eta(x)\eta(x')\rangle = \sigma^2\delta(x-x')$ and (3) $\varepsilon = \int_a^b f(x)\eta(x)\,\mathrm{d}x$, then ε is a real random number with $\langle\varepsilon\rangle = 0$ and covariance $\langle\varepsilon^2\rangle = \sigma^2\int_a^b f^2(x)\,\mathrm{d}x$ (Åström, 1970).

Using Result 1, we obtain $\langle\xi^n(t)\xi^n(t')\rangle = \sigma^2\delta(t-t')$.

In this work, the controlled variable is the surface covariance defined in Eq. (3). Without loss of generality, we pick $h_d(t) = 0$. Therefore, $\mathrm{Cov}_h(t)$ can be rewritten in terms of $\alpha_n(t)$ as follows (Lou and Christofides, 2005b):

$$\mathrm{Cov}_h(t) = \left\langle \int_{-\pi}^{\pi} [h(x,t) - 0]^2\,\mathrm{d}x \right\rangle = \left\langle \int_{-\pi}^{\pi} \left[\sum_{n=1}^{\infty} \alpha_n(t)\bar{\phi}_n(x)\right]^2 \mathrm{d}x \right\rangle$$
$$= \left\langle \sum_{n=1}^{\infty} \alpha_n(t)^2 \right\rangle = \sum_{n=1}^{\infty} \langle\alpha_n(t)^2\rangle \quad (9)$$

Eq. (9) provides a direct link between the surface covariance and the state covariance of the system of infinite stochastic ODEs of Eq. (6).

2.2. Model reduction

Owing to its infinite-dimensional nature, the system of Eq. (6) cannot be directly used as a basis for feedback controller design that can be implemented in practice (i.e., the practical implementation of such a controller will require the computation of infinite sums which cannot be done by a computer). Instead, we will use finite-dimensional approximations of the system of Eq. (6) for the purpose of model-based output feedback controller design. Specifically, we rewrite the system of Eq. (6) as follows:

$$\frac{\mathrm{d}x_s}{\mathrm{d}t} = \Lambda_s x_s + B_s u + \xi_s$$
$$\frac{\mathrm{d}x_f}{\mathrm{d}t} = \Lambda_f x_f + B_f u + \xi_f \quad (10)$$

where

$$x_s = [\alpha_1 \ \cdots \ \alpha_m]^{\mathrm{T}}, \quad x_f = [\alpha_{m+1} \ \alpha_{m+2} \ \cdots]^{\mathrm{T}}$$
$$\Lambda_s = \mathrm{diag}[\lambda_1 \ \cdots \ \lambda_m], \quad \Lambda_f = \mathrm{diag}[\lambda_{m+1} \ \lambda_{m+2} \ \cdots]$$
$$\xi_s = [\xi^1 \ \cdots \ \xi^m]^{\mathrm{T}}, \quad \xi_f = [\xi^{m+1}\,\xi^{m+2}\ldots]^{\mathrm{T}} \quad (11)$$

and

$$B_s = \begin{bmatrix} b_1^1 & \cdots & b_p^1 \\ \vdots & \ddots & \vdots \\ b_1^m & \cdots & b_p^m \end{bmatrix}, \quad B_f = \begin{bmatrix} b_1^{m+1} & \cdots & b_p^{m+1} \\ b_1^{m+2} & \cdots & b_p^{m+2} \\ \vdots & \vdots & \vdots \end{bmatrix} \quad (12)$$

Note that the x_s subsystem is mth-order and the x_f subsystem is infinite-dimensional.

The expression of Cov_h in Eq. (9) can be rewritten in the following form:

$$\mathrm{Cov}_h(t) = \sum_{n=1}^{m} \langle\alpha_n(t)^2\rangle + \sum_{n=m+1}^{\infty} \langle\alpha_n(t)^2\rangle$$
$$= \mathrm{Tr}[P_s(t)] + \mathrm{Tr}[P_f(t)] \quad (13)$$

where P_s and P_f are covariance matrices of x_s and x_f which are defined as $P_s = \langle x_s x_s^{\mathrm{T}}\rangle$ and $P_f = \langle x_f x_f^{\mathrm{T}}\rangle$, respectively. $\mathrm{Tr}[\cdot]$ denotes the trace of a matrix.

Neglecting the x_f subsystem, the following finite-dimensional approximation is obtained:

$$\frac{\mathrm{d}\tilde{x}_s}{\mathrm{d}t} = \Lambda_s\tilde{x}_s + B_s u + \xi_s \quad (14)$$

and the surface covariance of the infinite-dimensional stochastic system, Cov_h, can be approximated by $\widetilde{\mathrm{Cov}}_h$, which is computed from the state of the finite-dimensional approximation of Eq. (14) as follows:

$$\widetilde{\mathrm{Cov}}_h(t) = \mathrm{Tr}[\tilde{P}_s(t)] \tag{15}$$

where the tilde symbol denotes that the variable is associated with the finite-dimensional system. The reader may refer to Christofides and Daoutidis (1997), Theodotopoulou et al. (1998) and Christofides (2001) for further results on model reduction of dissipative PDEs.

2.3. State feedback control

When the state of the finite-dimensional system of Eq. (14) is available, a linear state feedback controller can be designed to regulate the surface covariance. The closed-loop finite-dimensional system takes the following form:

$$\begin{aligned} \frac{\mathrm{d}\tilde{x}_s}{\mathrm{d}t} &= \Lambda_s \tilde{x}_s + B_s u + \xi_s \\ u &= G\tilde{x}_s \end{aligned} \tag{16}$$

where G is the gain matrix, which should be carefully designed so as to stabilize the closed-loop finite-dimensional system and obtain the desired closed-loop surface covariance. Note that the linear state feedback controller of Eq. (16) has been used, in our previous work, to control the surface covariance in both thin film growth and ion-sputtering processes (Lou and Christofides, 2005a,b).

Since the above state feedback control assumes a full knowledge of the states of the process at all positions and times, which may be a restrictive requirement for certain practical applications, we proceed to design output feedback controllers by combining the state feedback control law and a state observer.

3. Output feedback control

In this section, we design linear output feedback controllers by combining the state feedback control law of Eq. (16) and a dynamic state observer which estimates the state of the finite-dimensional system of Eq. (14) using the measured process output with sensor noise. First, a dynamic state observer is developed using a Kalman–Bucy filter approach, which yields an optimal estimate of the state of the finite-dimensional system by minimizing the mean square estimation error. The dynamic state observer is then coupled to the state feedback controller of Eq. (16) to construct a dynamic output feedback controller. For the special case where the number of measurement sensors is equal to the order of the finite-dimensional system, a static output feedback controller may be designed by following a static state estimation approach proposed in Baker and Christofides (1999) and Christofides and Baker (1999).

3.1. Measured output with sensor noise

The state feedback controller of Eq. (16) requires the availability of the state $\tilde{x}_s$, which implies that the value of the surface height profile, $h(x,t)$, is available at any location and time. However, from a practical point of view, measurements of the surface height profile are only available at a finite number of locations. Motivated by this, we design an output feedback controller that uses measurements of the surface height at distinct locations to enforce a desired closed-loop surface covariance. The sensor noise is modeled as a Gaussian white noise and is added to the surface height measurements. Specifically, the measured process output is expressed as follows:

$$y(t) = [h(x_1,t) + \xi_y^1(t) \;\; h(x_2,t) + \xi_y^2(t) \;\; \cdots \;\; h(x_q,t) + \xi_y^q(t)]^{\mathrm{T}} \tag{17}$$

where x_i $(i = 1,2,\ldots,q)$ denotes a location of a point measurement sensor and q is the number of measurement sensors. $\xi_y^1(t)$, $\xi_y^2(t),\ldots,\xi_y^q(t)$ are independent Gaussian white noises with the following expressions for their means and covariances:

$$\begin{aligned} &\langle \xi_y^i(t) \rangle = 0, \quad i = 1,2,\ldots,q \\ &\langle \xi_y^i(t)\xi_y^j(t') \rangle = \varsigma^2 \delta_{ij}\delta(t-t'), \quad i = 1,2,\ldots,q, \;\; j = 1,2,\ldots,q \end{aligned} \tag{18}$$

where ς is a constant and δ_{ij} is the Kronecker delta function. Note that the sensor noises are independent of the system noises, ξ_s and ξ_f.

Using Eq. (5), the vector of measured outputs, $y(t)$, can be written in terms of x_s and x_f as follows:

$$\begin{aligned} y(t) &= \begin{bmatrix} \sum_{n=1}^{\infty} \alpha_n(t)\phi_n(x_1) + \xi_y^1(t) \\ \sum_{n=1}^{\infty} \alpha_n(t)\phi_n(x_2) + \xi_y^2(t) \\ \vdots \\ \sum_{n=1}^{\infty} \alpha_n(t)\phi_n(x_q) + \xi_y^q(t) \end{bmatrix} \\ &= C_s x_s(t) + C_f x_f(t) + \xi_y(t) \end{aligned} \tag{19}$$

where

$$\begin{aligned} C_s &= \begin{bmatrix} \phi_1(x_1) & \phi_2(x_1) & \cdots & \phi_m(x_1) \\ \phi_1(x_2) & \phi_2(x_2) & \cdots & \phi_m(x_2) \\ \vdots & \vdots & \ddots & \vdots \\ \phi_1(x_q) & \phi_2(x_q) & \cdots & \phi_m(x_q) \end{bmatrix} \\ C_f &= \begin{bmatrix} \phi_{m+1}(x_1) & \phi_{m+2}(x_1) & \cdots \\ \phi_{m+1}(x_2) & \phi_{m+2}(x_2) & \cdots \\ \vdots & \vdots & \ddots \\ \phi_{m+1}(x_q) & \phi_{m+2}(x_q) & \cdots \end{bmatrix} \end{aligned} \tag{20}$$

and

$$\xi_y(t) = [\xi_y^1(t) \;\; \xi_y^2(t) \;\; \cdots \;\; \xi_y^q(t)]^{\mathrm{T}} \tag{21}$$

Consequently, the system of Eq. (10) with the measured process output vector can be written as follows:

$$\begin{aligned} \frac{\mathrm{d}x_s}{\mathrm{d}t} &= \Lambda_s x_s + B_s u + \xi_s \\ \frac{\mathrm{d}x_f}{\mathrm{d}t} &= \Lambda_f x_f + B_f u + \xi_f \\ y &= C_s x_s + C_f x_f + \xi_y \end{aligned} \tag{22}$$

Neglecting the x_f subsystem, the following finite-dimensional stochastic ODE system can be obtained:

$$\begin{aligned} \frac{\mathrm{d}\tilde{x}_s}{\mathrm{d}t} &= \Lambda_s \tilde{x}_s + B_s u + \xi_s \\ \tilde{y} &= C_s \tilde{x}_s + \xi_y \end{aligned} \tag{23}$$

where the tilde symbols in $\tilde{x}_s$ and $\tilde{y}$ denote the correspondence to a reduced-order system. The system of Eq. (23) is used as the basis for output feedback controller design.

3.2. Dynamic output feedback control

To design a dynamic output feedback controller, we first construct a dynamic state estimator using information from the measured output vector. Specifically, a Kalman–Bucy filter is designed for the

optimal estimation of the state of the finite-dimensional system of Eq. (23) as follows (Hotz and Skelton, 1987):

$$\frac{d\hat{x}_s}{dt} = \Lambda_s\hat{x}_s + B_s u + K(y - C_s\hat{x}_s), \quad \hat{x}_s(0) = \hat{x}_{s0} \tag{24}$$

where $\hat{x}_s$ is the estimate of the state and K is a gain matrix, which is computed as follows (Hotz and Skelton, 1987):

$$K = QC_s^{\mathrm{T}}V_y^{-1} \tag{25}$$

where V_y is the sensor noise intensity matrix and satisfies

$$\langle \xi_y(t)\xi_y(t')^{\mathrm{T}}\rangle = V_y\delta(t - t') \tag{26}$$

and Q is the covariance matrix for the state estimation error and is defined as

$$Q = \lim_{t\to\infty}\langle \tilde{e}(t)\tilde{e}(t)^{\mathrm{T}}\rangle \tag{27}$$

where $\tilde{e}(t)$ is the estimation error:

$$\tilde{e} = \tilde{x}_s - \hat{x}_s. \tag{28}$$

The covariance matrix for the state estimation error, Q, is the unique nonnegative definite solution of the following algebraic Riccati equation (Hotz and Skelton, 1987):

$$\Lambda_s Q + Q\Lambda_s - QC_s^{\mathrm{T}}V_y^{-1}C_s Q + V_s = 0 \tag{29}$$

where V_s is the noise intensity matrix of the ξ_s and satisfies

$$\langle \xi_s(t)\xi_s(t')^{\mathrm{T}}\rangle = V_s\delta(t - t') \tag{30}$$

The dynamic output feedback controller is designed by combining the state feedback controller of Eq. (16) and the state estimator of Eq. (24) and takes the form

$$\begin{aligned}\frac{d\hat{x}_s}{dt} &= \Lambda_s\hat{x}_s + B_s u + K(y - C_s\hat{x}_s), \quad \hat{x}_s(0) = \hat{x}_{s0}\\ u &= G\hat{x}_s\end{aligned} \tag{31}$$

By applying the dynamic output feedback controller of Eq. (31) to the finite-dimensional system of Eq. (23), the following closed-loop finite dimensional system can be obtained:

$$\begin{aligned}\frac{d\tilde{x}_s}{dt} &= \Lambda_s\tilde{x}_s + B_s u + \xi_s\\ \tilde{y} &= C_s\tilde{x}_s + \xi_y\\ \frac{d\hat{x}_s}{dt} &= \Lambda_s\hat{x}_s + B_s u + K(\tilde{y} - C_s\hat{x}_s)\\ u &= G\hat{x}_s\end{aligned} \tag{32}$$

The closed-loop finite dimensional system of Eq. (32) can be written in terms of $\tilde{x}_s$ and e using Eq. (28) as follows:

$$\begin{aligned}\frac{d\tilde{x}_s}{dt} &= (\Lambda_s + B_s G)\tilde{x}_s - B_s G\tilde{e} + \xi_s\\ \frac{d\tilde{e}}{dt} &= (\Lambda_s - KC_s)\tilde{e} + \xi_s - K\xi_y\end{aligned} \tag{33}$$

The stability of the closed-loop finite-dimensional system of Eq. (33) depends on the stability properties of the matrices $(\Lambda_s + B_s G)$ and $(\Lambda_s - KC_s)$. Specifically, the stability of $(\Lambda_s + B_s G)$ depends on the appropriate design of the state feedback controller and the stability of $(\Lambda_s - KC_s)$ depends on the appropriate design of the Kalman–Bucy filter. Owing to its cascaded structure, the system of Eq. (33) is asymptotically stable if both $(\Lambda_s + B_s G)$ and $(\Lambda_s - KC_s)$ are stable matrices. A stable matrix is a matrix whose eigenvalues have all negative real part. This results in the existence of a steady-state covariance matrix (e.g., a covariance matrix as $t \to \infty$) of the closed-loop stochastic system (Hotz and Skelton, 1987). To investigate the steady-state covariance matrix of the closed-loop system of Eq. (33), we rewrite Eq. (33) as follows:

$$\frac{d}{dt}\begin{bmatrix}\tilde{x}_s\\ \tilde{e}\end{bmatrix} = \begin{bmatrix}\Lambda_s + B_s G & -B_s G\\ \mathbf{0} & \Lambda_s - KC_s\end{bmatrix}\begin{bmatrix}\tilde{x}_s\\ \tilde{e}\end{bmatrix} + \begin{bmatrix}I_s & \mathbf{0}\\ I_s & -K\end{bmatrix}\begin{bmatrix}\xi_s\\ \xi_y\end{bmatrix} \tag{34}$$

where I_s is an mth-order elementary matrix and $\mathbf{0}$ denotes a zero matrix with an appropriate size.

The steady-state covariance matrix of the system of Eq. (34) is defined as follows:

$$\tilde{P} = \lim_{t\to\infty}\left\langle\begin{bmatrix}\tilde{x}_s(t)\\ \tilde{e}(t)\end{bmatrix}[\tilde{x}_s(t)^{\mathrm{T}}\ \ \tilde{e}(t)^{\mathrm{T}}]\right\rangle = \begin{bmatrix}\tilde{P}_s & \tilde{P}_{se}\\ \tilde{P}_{es} & \tilde{P}_e\end{bmatrix} \tag{35}$$

where $\tilde{P}_s$, $\tilde{P}_e$, $\tilde{P}_{se}$ and $\tilde{P}_{es}$ are covariance matrices of the form

$$\begin{aligned}\tilde{P}_s &= \lim_{t\to\infty}\langle \tilde{x}_s(t)\tilde{x}_s(t)^{\mathrm{T}}\rangle\\ \tilde{P}_e &= \lim_{t\to\infty}\langle \tilde{e}(t)\tilde{e}(t)^{\mathrm{T}}\rangle\\ \tilde{P}_{se} &= \tilde{P}_{es}^{\mathrm{T}} = \lim_{t\to\infty}\langle \tilde{x}_s(t)\tilde{e}(t)^{\mathrm{T}}\rangle\end{aligned} \tag{36}$$

$\tilde{P}$ is the unique positive-definite solution of the following Lyapunov equation (Hotz and Skelton, 1987):

$$\begin{aligned}&\begin{bmatrix}\Lambda_s + B_s G & -B_s G\\ \mathbf{0} & \Lambda_s - KC_s\end{bmatrix}\tilde{P} + \tilde{P}\begin{bmatrix}\Lambda_s + B_s G & -B_s G\\ \mathbf{0} & \Lambda_s - KC_s\end{bmatrix}^{\mathrm{T}}\\ &\quad + \begin{bmatrix}I_s & \mathbf{0}\\ I_s & -K\end{bmatrix}\begin{bmatrix}V_s & \mathbf{0}\\ \mathbf{0} & V_y\end{bmatrix}\begin{bmatrix}I_s & \mathbf{0}\\ I_s & -K\end{bmatrix}^{\mathrm{T}} = \mathbf{0}\end{aligned} \tag{37}$$

When the solution of $\tilde{P}$ is available, the surface covariance of the finite-dimensional system, $\widetilde{\mathrm{Cov}}_h$, can be obtained by using only $\tilde{P}_s$.

Remark 1. The surface covariance of the closed-loop finite-dimensional system, $\widetilde{\mathrm{Cov}}_h$, under the linear output feedback controller of Eq. (31), can be solved from the Lyapunov equation of Eq. (37) with gain matrices G and K obtained from the separate designs of the state feedback control law of Eq. (16) and of the Kalman–Bucy filter of Eqs. (25) and (29). However, for a set-point regulation problem with a pre-specified desired surface covariance, $\widetilde{\mathrm{Cov}}_d$, the above procedure is not directly applicable. Instead, an iterative procedure can be adopted to design the matrices G and K to approach a desired set-point in the closed-loop system. Specifically, the state feedback controller can be first designed so that the set-point value can be achieved when the full state of the finite-dimensional system is accessible by the controller (see Section 3.2 in Lou and Christofides, 2005a, for more details on the state feedback gain design). This design will result in a control gain matrix, G_1 in the state feedback controller. Then, a Kalman filter can be designed separately to compute the Kalman filter gain matrix, K_1, by solving the Riccati equation. Subsequently, the surface covariance under the resulting output feedback controller (K_1, G_1), $\widetilde{\mathrm{Cov}}_{h,1}$, can be obtained by solving the Lyapunov equation of Eq. (37). Due to the fact that less information of the surface state is used in the output feedback controller compared to the corresponding state feedback controller, estimation error always exists. Therefore, the closed-loop surface covariance, $\widetilde{\mathrm{Cov}}_{h,1}$, will be different from the set-point value, $\widetilde{\mathrm{Cov}}_d$. To enable the use of an iterative procedure to improve upon $\widetilde{\mathrm{Cov}}_{h,1}$, a second set-point value for surface covariance, $\widetilde{\mathrm{Cov}}_{d,2}$, is used to solve for another pair of gain matrices G_2 and K_2. A new $\widetilde{\mathrm{Cov}}_{h,2}$ under the output feedback controller with gain matrices G_2 and K_2 is then obtained, which results in a different closed-loop surface covariance, $\widetilde{\mathrm{Cov}}_{h,2}$. With the two sets of data as initial guesses, we can start an iterative procedure using, for example, Secant's method to solve for K_i, G_i that results in a closed-loop surface covariance, $\widetilde{\mathrm{Cov}}_{h,i}$, sufficiently close to the desired surface covariance, $\widetilde{\mathrm{Cov}}_d$.

The iterative procedure terminates when the difference between the closed-loop finite-dimensional surface covariance under output feedback control is sufficiently close to the desired value $\widetilde{\mathrm{Cov}}_d$.

3.3. Analysis of closed-loop infinite-dimensional system

We now proceed to characterize the accuracy with which the surface covariance in the closed-loop infinite-dimensional system is controlled by the finite-dimensional linear dynamic output feedback controller. By applying the controller of Eq. (31) to the infinite-dimensional system of Eq. (10) and substituting the estimation error in Eq. (28), the infinite-dimensional closed-loop system takes the following form:

$$\begin{aligned}\frac{\mathrm{d}x_s}{\mathrm{d}t} &= (\Lambda_s + B_s G)x_s - B_s G e + \xi_s\\ \frac{\mathrm{d}e}{\mathrm{d}t} &= (\Lambda_s - KC_s)e - KC_f x_f + \xi_s - K\xi_y\\ \varepsilon\frac{\mathrm{d}x_f}{\mathrm{d}t} &= \Lambda_{f\varepsilon}x_f + \varepsilon(B_f G x_s - B_f G e) + \varepsilon\xi_f\end{aligned} \tag{38}$$

where e is the estimation error from the full-order system and is defined as $e = x_s - \hat{x}_s$, $\varepsilon = |\lambda_1|/|\lambda_{m+1}|$, and $\Lambda_{f\varepsilon} = \varepsilon\Lambda_f$ is an infinite-dimensional stable matrix.

The infinite-dimensional system of Eq. (38) is then a singularly-perturbed system driven by white noise. We now proceed to characterize the accuracy with which the surface covariance is controlled in the closed-loop infinite-dimensional system. Theorem 1 provides a characterization of the surface covariance enforced by the dynamic output feedback controller in the closed-loop infinite dimensional system. The proof of Theorem 1 is given in Appendix.

Theorem 1. *Consider the surface covariance of the finite-dimensional system of Eq.* (33), $\widetilde{\mathrm{Cov}}_h$

$$\tilde{P}_s = \lim_{t\to\infty}\langle\tilde{x}_s(t)\tilde{x}_s(t)^{\mathrm{T}}\rangle, \quad \widetilde{\mathrm{Cov}}_h = \mathrm{Tr}\{\tilde{P}_s\} \tag{39}$$

and the surface covariance of the infinite-dimensional system of Eq. (38), Cov_h

$$x = [x_s^{\mathrm{T}}\ x_f^{\mathrm{T}}]^{\mathrm{T}}, \quad P = \lim_{t\to\infty}\langle x(t)x(t)^{\mathrm{T}}\rangle, \ \mathrm{Cov}_h = \mathrm{Tr}\{P\} \tag{40}$$

where $\langle\cdot\rangle$ *denotes the expected value. Then, there exists* $\varepsilon^* > 0$ *such that if* $\varepsilon \in (0, \varepsilon^*]$, $\widetilde{\mathrm{Cov}}_h$ *and* Cov_h *satisfy*

$$\mathrm{Cov}_h = \widetilde{\mathrm{Cov}}_h + O(\sqrt{\varepsilon}) \tag{41}$$

Remark 2. The minimum number of sensors required for the operation of the Kalman–Bucy filter is the number that satisfies the observability requirement of the system, which is typically a small number. If more measurement sensors are available, it may result in improved state estimation and closed-loop performance since more information of the surface profile is available for state estimation. However, a small number of measurement sensors is favorable in many applications when the cost and complexity of the overall control system is a concern. Further discussion regarding the selection of measurement sensors is provided in the simulation section.

Remark 3. In the special case where the number of sensors is equal to the order of the x_s subsystem, i.e., $q = m$, a static output feedback controller can be designed, by following the state estimation method developed in Baker and Christofides (1999), Christofides and Baker (1999) and Christofides (2001), to estimate the state of the finite-dimensional system, $\tilde{x}_s$, directly from the measured output, y, and the resulting static output feedback controller takes the form

$$\begin{aligned}\hat{x}_s &= C_s^{-1}y\\ u &= G\hat{x}_s\end{aligned} \tag{42}$$

Note that the same state feedback control law of Eq. (16) is used in the static output feedback controller of Eq. (42).

4. Simulation results

In this section, we first present applications of the proposed linear output feedback covariance controller to the linearized stochastic KSE to demonstrate the effectiveness of the proposed output feedback covariance controllers. Then, both linear and nonlinear covariance control of the nonlinear stochastic KSE are considered. A nonlinear output feedback covariance controller is first developed by combining the linear state feedback control law and a nonlinear state observer and is applied to the nonlinear stochastic KSE. Finally, nonlinear state feedback controller and nonlinear output feedback controller designs are presented and applied to the nonlinear KSE.

4.1. The linearized stochastic KSE

The stochastic KSE is a fourth-order nonlinear stochastic partial differential equation that describes the evolution of the height fluctuation for surfaces in a variety of material preparation processes including surface erosion by ion sputtering (Cuerno et al., 1995; Lauritsen et al., 1996), surface smoothing by energetic clusters (Insepov et al., 1997) and ZrO_2 thin film growth by reactive ion beam sputtering (Qi et al., 2003). The linearized stochastic KSE around the zero solution ($h(x,t) = 0$) takes the following form:

$$\begin{aligned}\frac{\partial h}{\partial t} &= -\frac{\partial^2 h}{\partial x^2} - \kappa\frac{\partial^4 h}{\partial x^4} + \sum_{i=1}^{p} b_i(x)u_i(t) + \xi(x,t)\\ y(t) &= [h(x_1,t) + \xi_y^1(t)\ \ h(x_2,t) + \xi_y^2(t)\ \ \cdots\ \ h(x_q,t) + \xi_y^q(t)]^{\mathrm{T}}\end{aligned} \tag{43}$$

subject to periodic boundary conditions

$$\frac{\partial^j h}{\partial x^j}(-\pi,t) = \frac{\partial^j h}{\partial x^j}(\pi,t), \quad j = 0,\ldots,3 \tag{44}$$

and the initial condition $h(x,0)=h_0(x)$, where $x \in [-\pi,\pi]$ is the spatial coordinate and $\kappa > 0$ is the instability parameter of the stochastic KSE.

The eigenvalue problem of the linear operator of Eq. (43) takes the form

$$\begin{aligned}\mathscr{A}\bar{\phi}_n(x) &= -\frac{\mathrm{d}^2\bar{\phi}_n(x)}{\mathrm{d}x^2} - \kappa\frac{\mathrm{d}^4\bar{\phi}_n(x)}{\mathrm{d}x^4} = \lambda_n\bar{\phi}_n(x)\\ \frac{\mathrm{d}^j\bar{\phi}_n}{\mathrm{d}x^j}(-\pi) &= \frac{\mathrm{d}^j\bar{\phi}_n}{\mathrm{d}x^j}(+\pi), \quad j = 0,\ldots,3, \ \ n = 1,\ldots,\infty\end{aligned} \tag{45}$$

A direct computation of the solution of the above eigenvalue problem yields $\lambda_0 = 0$ with $\psi_0 = 1/\sqrt{2\pi}$, and $\lambda_n = n^2 - \kappa n^4$ (λ_n is an eigenvalue of multiplicity two) with eigenfunctions $\phi_n = (1/\sqrt{\pi})\sin(nx)$ and $\psi_n = (1/\sqrt{\pi})\cos(nx)$ for $n = 1,\ldots,\infty$. Note that the $\bar{\phi}_n$ in the general eigenvalue problem formulation of Eq. (4) denotes either ϕ_n or ψ_n. From the expression of the eigenvalues, it follows that for a fixed value of $\kappa > 0$, the number of unstable eigenvalues of the operator $\mathscr{A}$ in Eq. (45) is finite and the distance between two consecutive eigenvalues (i.e., λ_n and λ_{n+1}) increases as n increases.

For $0 < \kappa < 1$, the operator of Eq. (4) possesses unstable eigenvalues. Thus, the zero solution of the open-loop system of Eq. (43) is unstable, which implies that the surface covariance increases with time due to the open-loop instability of the zero solution. An appropriately designed feedback controller is necessary to regulate the surface covariance to a desired value.

Using modal decomposition, the linearized stochastic KSE is formulated into an infinite-dimensional stochastic ODE system as follows:

$$\frac{d\alpha_n}{dt} = (n^2 - \kappa n^4)\alpha_n + \sum_{i=1}^{p} b_{i\alpha_n} u_i(t) + \xi_\alpha^n(t), \quad n = 1, \ldots, \infty$$
$$\frac{d\beta_n}{dt} = (n^2 - \kappa n^4)\beta_n + \sum_{i=1}^{p} b_{i\beta_n} u_i(t) + \xi_\beta^n(t), \quad n = 0, 1, \ldots, \infty \qquad (46)$$

A finite-dimensional approximation of Eq. (46) can be then derived by neglecting the fast modes (i.e., modes of order $m+1$ and higher) and a system of the form of Eq. (14) is obtained for covariance controller design.

A linear state feedback controller is initially designed on the basis of the finite-dimensional approximation by following the method proposed by Lou and Christofides (2005a), which takes the following form:

$$u = B_s^{-1}(\Lambda_{cs} - \Lambda_s)\tilde{x}_s \qquad (47)$$

where the matrix Λ_{cs} contains the desired poles of the closed-loop system; $\Lambda_{cs} = \text{diag}[\lambda_{c\beta 0}\ \lambda_{c\alpha 1}\ \cdots\ \lambda_{c\alpha m}\ \lambda_{c\beta 1}\ \cdots\ \lambda_{c\beta m}]$. $\lambda_{c\beta 0}$, $\lambda_{c\alpha i}$ and $\lambda_{c\beta i}$ $(i = 1, \ldots, m)$ are desired poles of the closed-loop finite-dimensional system, which satisfy $Re\{\lambda_{c\alpha i}\} < 0$ for $i = 1, \ldots, m$ and $Re\{\lambda_{c\beta i}\} < 0$ for $i = 0, 1, \ldots, m$. By applying the controller in Eq. (47), the dynamics of the closed-loop finite-dimensional system is fully described by the matrix Λ_{cs}.

To simplify the development, we assume that $p = 2m+1$ (i.e., the number of control actuators is equal to the dimension of the finite dimensional system) and pick the actuator distribution functions, $b_i(x)$, to have the following form:

$$b_i(x) = \begin{cases} \dfrac{1}{\sqrt{2\pi}}, & i = 1 \\ \dfrac{1}{\sqrt{\pi}} \sin[(i-1)x], & i = 2, \ldots, m+1 \\ \dfrac{1}{\sqrt{\pi}} \cos[(i-m-1)x], & i = m+2, \ldots, 2m+1 \end{cases} \qquad (48)$$

Note that the actuator distribution functions are selected such that B_s^{-1} exists. The following parameters are used in the simulation:

$$\kappa = 0.1, \quad \sigma = 1.0, \quad \varsigma = 0.1, \quad m = 5 \qquad (49)$$

We design the linear state feedback controller such that all the desired poles in Λ_{cs} are equal to -10.0. The surface covariance of the infinite-dimensional system under the state feedback controller is 0.55. The method to determine the values of the closed-loop poles to regulate the surface covariance to a set-point value can be found in Lou and Christofides (2005a) and is omitted here for brevity.

Eleven measurement sensors are used and are evenly placed on the spatial domain $[-\pi, \pi]$. A perfect initial surface is assumed and zero initial state estimates are used for all simulations:

$$h_0(x) = 0, \quad x_s(0) = \hat{x}_s(0) = \mathbf{0}, \quad x_f(0) = \mathbf{0} \qquad (50)$$

A 50th order stochastic ODE approximation of Eq. (43) is used to simulate the process. The stochastic ODEs are solved using Euler–Maruyama approximation with time discretization size of $\Delta t = 10^{-4}$. The choices of the truncation order and time discretization size lead to the convergence of the solution. Since it is a stochastic process, the surface covariance profile is obtained by averaging the results of 1000 independent simulation runs using the same parameters to produce a smooth profile of surface covariance evolution.

Remark 4. In this work, the sensors are uniformly placed in the whole spatial domain and the simulation results show that this is a good choice in the sense that the placement results in good closed-loop performance under output feedback control. In general, the optimal sensor placement should be determined so that the state estimation error is minimized. A systematic solution for the problem for optimal sensor placement for stochastic distributed parameter systems is current lacking but is outside of the scope of the current work.

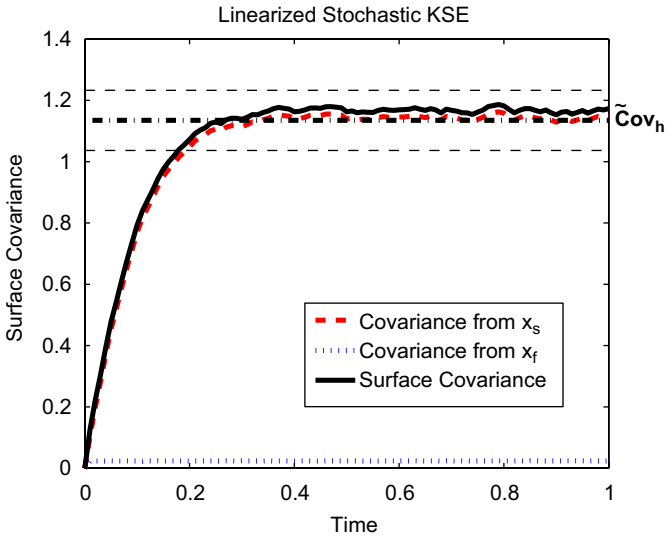

Fig. 1. The closed-loop surface covariance under linear dynamic output feedback control using 11 measurement sensors. The horizontal dashed lines represent the range in which the surface covariance Cov_h is expected to be based on the theoretical estimates of Theorem 1.

4.2. Linear dynamic output feedback control of linearized stochastic KSE

In the closed-loop simulation under linear dynamic output feedback control, a Kalman–Bucy filter is designed to estimate the state of the finite-dimensional system. The gain matrix K is obtained from the solution of the algebraic Riccati equation of Eqs. (25) and (29). $\widetilde{\text{Cov}}_h$ is the surface covariance of the closed-loop finite-dimensional system under the finite-dimensional output feedback covariance controller and is the solution of the Lyapunov equation of Eq. (37). According to Theorem 1, $\widetilde{\text{Cov}}_h$ is an $O(\sqrt{\varepsilon})$ approximation of the closed-loop surface covariance of the infinite-dimensional system, Cov_h, i.e., the closed-loop surface covariance of the infinite-dimensional system is an $O(\sqrt{\varepsilon})$ approximation of the desired value. To regulate the surface covariance to a desired value, the ε should be sufficiently small, which can be achieved by appropriately selecting the size of the finite-dimensional approximation used for covariance controller design. In this design, when $m = 5$, $\varepsilon = 0.01$, which is a sufficiently small number compared to the desired closed-loop surface covariance.

Since we use 11 measurement sensors, $q = 2m + 1$ and the observer gain matrix is a square matrix. The desired surface covariance is 1.1347. Based on this desired surface covariance, the gain matrices for both the state observer, K, and the state feedback control law, G, are determined via the iterative procedure of Remark 1. Note that because of the existence of the sensor noise, the surface covariance under the output feedback covariance controller is higher than the one under state feedback control where the same gain matrix, G, is used and the full state of the surface is accessible. The closed-loop simulation result under the dynamic output feedback controller with 11 measurement sensors is shown in Fig. 1. The controller successfully drives the surface covariance of the closed-loop infinite-dimensional system to a level which is within the range of the theoretical estimate of Theorem 1, i.e., $\sqrt{\varepsilon} \simeq 0.1$ and $\text{Cov}_h = \widetilde{\text{Cov}}_h + O(0.1)$.

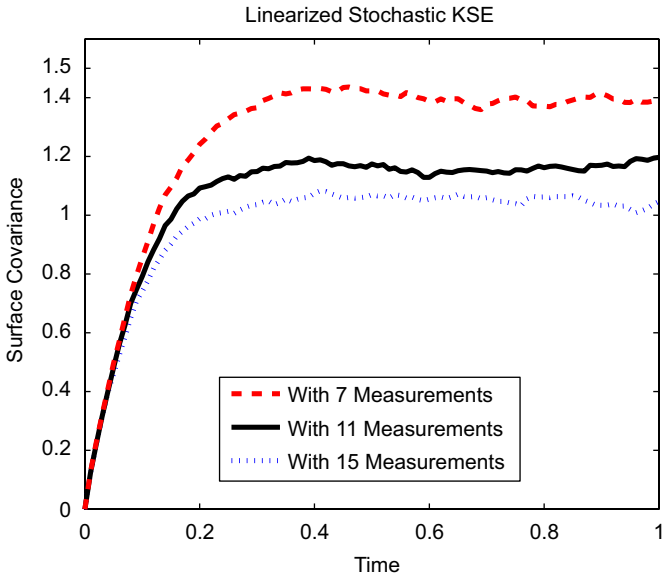

Fig. 2. Comparison of the surface covariance under linear dynamic output feedback controllers with 7, 11 and 15 measurement sensors.

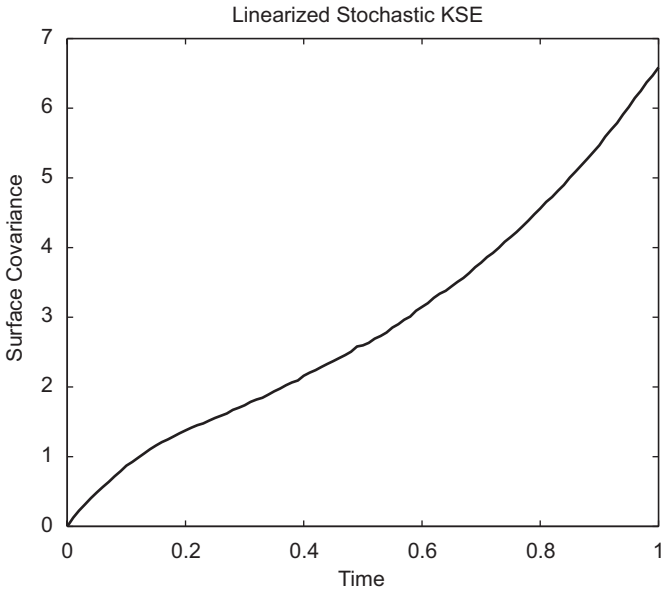

Fig. 3. The closed-loop profile of the surface covariance under linear dynamic output feedback control with six measurement sensors.

The result shown in Fig. 1 also confirms that the surface covariance contribution from the x_f subsystem is negligible and that the contribution from the x_s subsystem is dominant. Therefore, the design of the output feedback covariance controller based on the x_s subsystem can regulate the surface covariance of the infinite-dimensional closed-loop system to the desired level.

For dynamic output feedback control design, the number of the measurements is not needed to be equal to the dimension of the finite-dimensional system. A number of measurement sensors that is larger than the dimension of the finite-dimensional system results in a more accurate state estimation from the Kalman–Bucy filter. Therefore, the closed-loop surface covariance can be closer to the set-point value compared to the one in which the number of measurement sensors is equal to the dimension of the finite-dimensional system. On the other hand, when the number of the measurement sensors is smaller than the dimension of the finite-dimensional system but is equal to or larger than the number of unstable modes of the system, it is still possible to design a stable Kalman–Bucy filter for state estimation. Fig. 2 shows the comparison of closed-loop simulation results when different numbers of measurement sensors are used for state estimation. The feedback control law is the same for all simulations. Specifically, Fig. 2 shows results from three closed-loop simulation runs with 7, 11 and 15 measurement sensors. It is clear that the control system which uses a larger number of measurement sensors is capable of controlling the surface covariance to a lower level. On the other hand, since the dimension of the finite-dimensional system is 11, it is possible to stabilize the surface covariance to a finite value when the number of measurement sensors is smaller than the dimension of the finite-dimensional system.

However, there is a minimum number of measurement sensors required by the dynamic output feedback controller to stabilize the system. In this study, a minimum of seven measurement sensors are required. When the number of measurement sensors is fewer than the minimum number, seven, the output feedback controller cannot stabilize the closed-loop system. In Fig. 3, we show the closed-loop simulation result under a linear dynamic output feedback controller using six measurement sensors. The surface covariance of the closed-loop system under such a controller is not stabilized to a finite value.

4.3. Dynamic output feedback control of nonlinear stochastic KSE

In this subsection, the application of dynamic output feedback controllers to the nonlinear stochastic KSE is considered. We first formulate the nonlinear stochastic KSE into an infinite-dimensional nonlinear stochastic ODE system and a finite-dimensional approximation is derived as a basis for controller design. In addition to the linear output feedback controller, a nonlinear dynamic output feedback controller is also designed by combining a nonlinear state feedback controller developed in our previous work (Lou and Christofides, 2006) and an appropriate nonlinear state estimator. Both linear and nonlinear dynamic output feedback controllers are applied to the nonlinear stochastic KSE and the closed-loop performance under both controllers is compared.

The nonlinear stochastic KSE with distributed control and measured output with sensor noise takes the following form:

$$\frac{\partial h}{\partial t} = -\frac{\partial^2 h}{\partial x^2} - \kappa\frac{\partial^4 h}{\partial x^4} + \left(\frac{\partial h}{\partial x}\right)^2 + \sum_{i=1}^{p} b_i(x)u_i(t) + \xi(x,t)$$
$$y(t) = [h(x_1,t) + \xi_y^1(t)\ \ h(x_2,t) + \xi_y^2(t)\ \ \cdots\ \ h(x_q,t) + \xi_y^q(t)]^{\mathrm{T}} \qquad (51)$$

subject to periodic boundary conditions

$$\frac{\partial^j h}{\partial x^j}(-\pi,t) = \frac{\partial^j h}{\partial x^j}(\pi,t), \quad j = 0,\ldots,3 \qquad (52)$$

and the initial condition

$$h(x,0) = h_0(x) \qquad (53)$$

The variables are defined in the same way as those in Eq. (43). Following a similar approach to the one presented in Section 4.1, the following system of infinite nonlinear stochastic ODEs with distributed

control can be obtained:

$$\frac{d\alpha_n}{dt} = (n^2 - \kappa n^4)\alpha_n + f_{n\alpha} + \sum_{i=1}^{p} b_{i\alpha_n} u_i(t) + \xi_\alpha^n(t), \quad n = 1, \ldots, \infty$$
$$\frac{d\beta_n}{dt} = (n^2 - \kappa n^4)\beta_n + f_{n\beta} + \sum_{i=1}^{p} b_{i\beta_n} u_i(t) + \xi_\beta^n(t), \quad n = 0, 1, \ldots, \infty \tag{54}$$

where

$$f_{n\alpha} = \int_{-\pi}^{\pi} \phi_n(x) \times \left(\sum_{j=1}^{\infty} \alpha_j(t) \frac{d\phi_j}{dx}(x) + \sum_{j=0}^{\infty} \beta_j(t) \frac{d\psi_j}{dx}(x) \right)^2 dx$$
$$f_{n\beta} = \int_{-\pi}^{\pi} \psi_n(x) \times \left(\sum_{j=1}^{\infty} \alpha_j(t) \frac{d\phi_j}{dx}(x) + \sum_{j=0}^{\infty} \beta_j(t) \frac{d\psi_j}{dx}(x) \right)^2 dx \tag{55}$$

The system of Eq. (54) can be rewritten in the following form with the measured output:

$$\frac{dx_s}{dt} = \Lambda_s x_s + f_s(x_s, x_f) + B_s u + \xi_s$$
$$\frac{dx_f}{dt} = \Lambda_f x_f + f_f(x_s, x_f) + B_f u + \xi_f$$
$$y = C_s x_s + C_f x_f + \xi_y \tag{56}$$

Note that the dimension of the x_s subsystem is $2m + 1$ and the x_f subsystem is infinite-dimensional.

In the closed-loop simulation of the nonlinear stochastic KSE, we use the same actuator distribution functions, same value of the model parameter, κ, and same initial conditions as those used in the closed-loop simulation of the linearized stochastic KSE. The linear dynamic output feedback controller developed in Section 4.2 is applied to the nonlinear stochastic KSE using 11 measurement sensors. A 50th order stochastic ODE approximation of Eq. (43) is used to simulate the nonlinear process.

The closed-loop simulation result of the nonlinear stochastic KSE under the linear dynamic output feedback controller is shown in Fig. 4. The surface covariance is stabilized to a finite-value under the linear output feedback covariance controller, since the controller is designed to stabilize the linear part of the system of Eq. (22). Therefore, when we apply the linear controller to the nonlinear system, the closed-loop system is locally stable. Although the nonlinear system is stabilized, there is a relatively big error between the closed-loop surface covariance and the set-point value, $\widetilde{\text{Cov}}_h$. As shown in Fig. 4, this error is outside of the approximation error boundaries, $O(\sqrt{\varepsilon})$, and thus it is not due to the use of a finite-dimensional approximation of the stochastic KSE for control design. This error is due to the nonlinearity of the system, which is not explicitly accounted for in the controller design. Therefore, a nonlinear controller is necessary to improve the closed-loop performance.

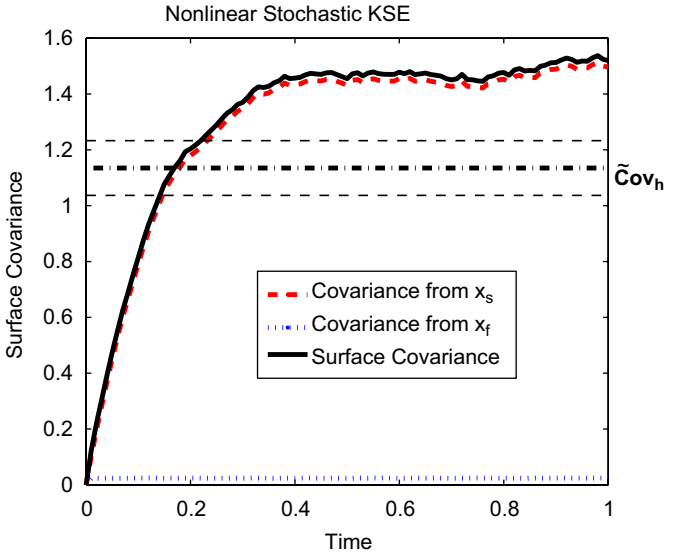

Fig. 4. The closed-loop surface covariance profile of the nonlinear stochastic KSE under linear dynamic output feedback control with 11 measurement sensors. The horizontal dashed lines represent the range in which the surface covariance Cov_h is expected to be based on the theoretical estimates of Theorem 1.

4.3.1. Nonlinear state feedback control design

In this subsection, the goal is to design a nonlinear output feedback controller which explicitly accounts for the nonlinearity of the stochastic KSE model of Eq. (51). Neglecting the x_f subsystem, the following $2m$-dimensional system is obtained:

$$\frac{d\tilde{x}_s}{dt} = \Lambda_s \tilde{x}_s + f_s(\tilde{x}_s, 0) + B_s u + \xi_s \tag{57}$$

where the tilde symbol denotes that the state variable is associated with a finite-dimensional system.

Following the method proposed in our previous work (Lou and Christofides, 2006), a nonlinear state feedback controller is first designed on the basis of the finite-dimensional approximation of Eq. (57) as follows:

$$u = B_s^{-1}\{(\Lambda_{cs} - \Lambda_s)\tilde{x}_s - f_s(\tilde{x}_s, 0)\} \tag{58}$$

Note that the nonlinear term, $f_s(\tilde{x}_s, 0)$, is explicitly accounted for in the nonlinear controller design. The choice of Λ_{cs} is similar to the choice in Eq. (47) and determines the dynamics of the closed-loop finite-dimensional system.

Under the nonlinear state feedback controller, the closed-loop finite-dimensional system is an approximate ($O(\sqrt{\varepsilon})$ approximation) linear stochastic system (see the proof of Theorem 1 in Lou and Christofides, 2006). The steady-state surface covariance of the closed-loop finite-dimensional system under the nonlinear state feedback controller can be obtained by following the method presented in Section 3.1. An analysis of the performance of the closed-loop nonlinear infinite-dimensional system enforced by the nonlinear state feedback controller of Eq. (58) can also been found in Lou and Christofides (2006). To show the effectiveness of the nonlinear state feedback controller, we apply both the linear state feedback controller of Eq. (47) and the nonlinear state feedback controller of Eq. (58) to the nonlinear stochastic KSE. The results are presented in Fig. 5. Both the linear and nonlinear state feedback controllers stabilize the surface covariance to a finite value. However, the steady state surface covariance under the nonlinear controller is much closer to the set-point value compared to the one under the linear controller. The nonlinear state feedback controller successfully drives the surface covariance of the closed-loop infinite-dimensional system of nonlinear KSE to the set-point value $\widetilde{\text{Cov}}_h$, which is within the range of the theoretical estimate (for the theoretical estimation of the surface covariance of the closed-loop infinite-dimensional nonlinear system under the nonlinear state feedback controller, see Theorem 1 in Lou and Christofides, 2006). The surface covariance under the linear state feedback controller falls outside of the range of the theoretical estimate. The improved performance of the nonlinear state feedback controller is due to the

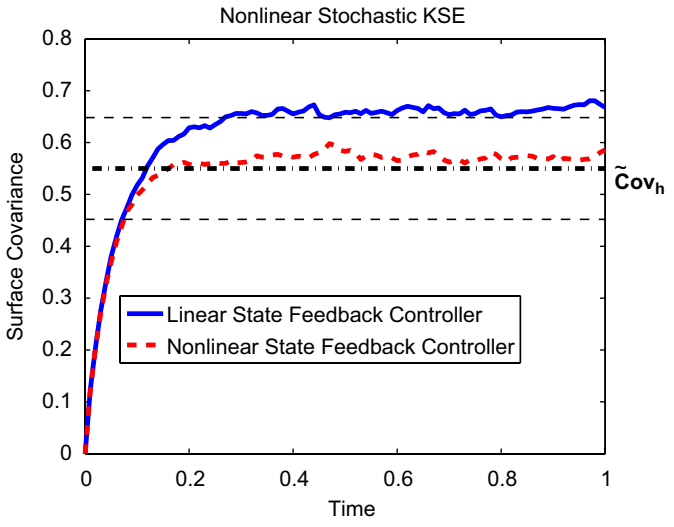

Fig. 5. Comparison of the closed-loop surface covariance profiles of the nonlinear stochastic KSE under linear and nonlinear state feedback control. The horizontal dashed lines represent the range in which the surface covariance Cov_h is expected to be based on the theoretical estimates of Theorem 1 in Lou and Christofides (2006).

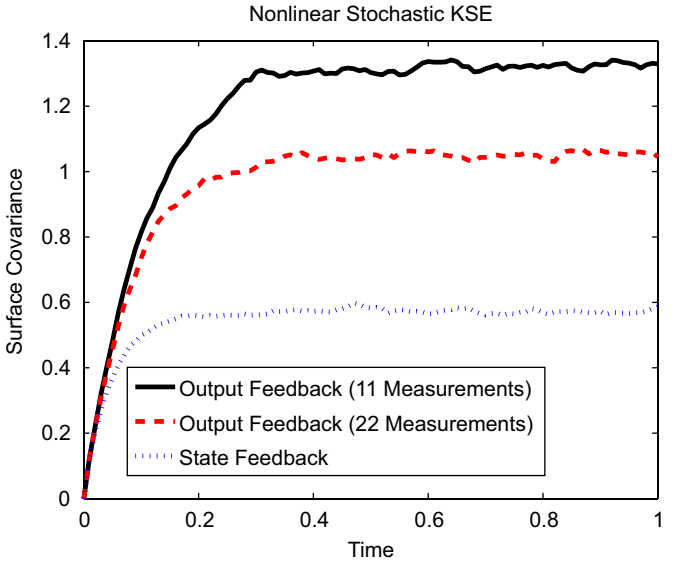

Fig. 6. The surface covariance of nonlinear KSE under nonlinear dynamic output feedback controls with different numbers of measurement sensors.

fact that the nonlinearity of the process model is explicitly accounted for in the controller design.

4.3.2. Nonlinear dynamic output feedback control of nonlinear stochastic KSE

In this subsection, we design a nonlinear dynamic output feedback controller by combining the nonlinear state feedback controller of Eq. (58) and a dynamic nonlinear state estimator. An appropriate nonlinear state estimator is considered of the form

$$\frac{d\hat{x}_s}{dt} = \Lambda_s \hat{x}_s + f_s(\hat{x}_s, 0) + B_s u + K(y - C_s \hat{x}_s) \tag{59}$$

where the gain matrix, K, is determined by using Eq. (25).

The resulting nonlinear dynamic output feedback controller takes then the form

$$\frac{d\hat{x}_s}{dt} = \Lambda_s \hat{x}_s + f_s(\hat{x}_s, 0) + B_s u + K(y - C_s \hat{x}_s), \quad \hat{x}_s(0) = \hat{x}_{s0}$$
$$u = B_s^{-1}\{(\Lambda_{cs} - \Lambda_s)\hat{x}_s - f_s(\hat{x}_s, 0)\} \tag{60}$$

Fig. 6 shows the surface covariance profiles of the closed-loop system under nonlinear dynamic output feedback control with different numbers of measurement sensors. For comparison, the closed-loop surface covariance under the nonlinear state feedback controller is also shown in Fig. 6. There are differences between the steady-state surface covariance under the nonlinear dynamic output feedback controller and under the state feedback controller. A higher number of measurement sensors leads to a smaller difference since more information of the surface is available to the state estimator. This is consistent with the fact that a higher number of measurement sensors is capable of achieving a lower closed-loop surface covariance under output feedback covariance control. Note that the state feedback controller gives the lowest steady-state surface covariance since there is no estimation error involved in its implementation.

5. Conclusions

In this work, we developed a method for dynamic output feedback covariance control of the state covariance of linear dissipative stochastic PDEs using spatially distributed control actuation and sensing with measurement noise. The stochastic PDE was initially formulated into a system of infinite stochastic ODEs by using modal decomposition. A finite-dimensional approximation was then obtained to capture the dominant mode contribution to the surface roughness profile (i.e., the covariance of the surface height profile). Subsequently, a state feedback controller and a Kalman–Bucy filter were designed on the basis of the finite-dimensional approximation. The resulting linear dynamic output feedback controller is the one that couples the state feedback controller and the state estimator. The steady-state expected surface covariance under the linear dynamic output feedback controller was then estimated on the basis of the closed-loop finite-dimensional system. An analysis was performed to obtain an estimate of the expected surface covariance of the closed-loop infinite-dimensional system. Applications of the linear dynamic output feedback controller to the linearized and nonlinear stochastic Kuramoto–Sivashinsky equations were presented. Finally, nonlinear state feedback controller and nonlinear output feedback controller designs were also presented and applied to the nonlinear KSE.

Acknowledgment

Financial support from NSF, CBET-0652131, is gratefully acknowledged by Gangshi Hu and Panagiotis D. Christofides.

Appendix

Proof of Theorem 1. The proof of Theorem 1 includes several steps. First, we prove that the closed-loop infinite-dimensional system of Eq. (38) is exponentially stable for sufficiently small ε. Second, we prove that the contribution to the surface covariance from the x_f subsystem of Eq. (38) is $O(\varepsilon)$, i.e.,

$$Cov_{hf} = \mathrm{Tr}\{P_f\} = O(\varepsilon) \tag{61}$$

where Cov_{hf} is the contribution to the surface covariance from the x_f subsystem of Eq. (38) and P_f is the covariance matrix defined as

$$P_f = \lim_{t\to\infty} \langle x_f(t) x_f(t)^{\mathrm{T}} \rangle \tag{62}$$

Then, we prove that the contribution to the surface covariance from the x_s subsystem of Eq. (38) is as follows:

$$Cov_{hs} = \mathrm{Tr}\{P_s\} = Cov_h + O(\sqrt{\varepsilon}) \tag{63}$$

where Cov_h, defined in Eq. (15), is the surface covariance of the closed-loop finite-dimensional system of Eq. (33), and P_s is the covariance matrix of x_s in Eq. (38), which is defined as

$$P_s = \lim_{t\to\infty} \langle x_s(t) x_s(t)^{\mathrm{T}} \rangle \tag{64}$$

Finally, the proof of Theorem 1 is completed by proving Eq. (41) based on the results in Eqs. (61) and (63).

Closed-loop infinite dimensional system stability. Referring to the closed-loop infinite-dimensional system of Eq. (38), we note that the fast subsystem (obtained by rewriting the system of Eq. (38) in the fast time scale $\tau = t/\varepsilon$ and setting $\varepsilon = 0$) takes the form

$$\frac{\mathrm{d}\bar{x}_f}{\mathrm{d}\tau} = \Lambda_{f\varepsilon}\bar{x}_f \tag{65}$$

Due to the eigenspectrum of the linear operator of Eq. (1), all eigenvalues of $\Lambda_{f\varepsilon}$ have negative real parts. Thus, the system of Eq. (65) is exponentially stable. Setting $\varepsilon = 0$ in the system of Eq. (38), the closed-loop finite dimensional system is obtained:

$$\begin{aligned} \frac{\mathrm{d}\tilde{x}_s}{\mathrm{d}t} &= (\Lambda_s + B_s G)\tilde{x}_s - B_s G\tilde{e} + \xi_s \\ \frac{\mathrm{d}\tilde{e}}{\mathrm{d}t} &= (\Lambda_s - KC_s)\tilde{e} + \xi_s - K\xi_y \end{aligned} \tag{66}$$

which is exponentially stable since the matrices $(\Lambda_s + B_s G)$ and $(\Lambda_s - KC_s)$ are stable matrices by design. Therefore, there exists (following similar arguments to Kokotovic et al., 1986, Theorem A.1, p. 361) a positive real number $\hat{\varepsilon}$ such that $\forall \varepsilon \in (0, \hat{\varepsilon}]$, the zero solution of the closed-loop infinite-dimensional system of Eq. (38) is exponentially stable. □

Proof of Eq. (61). We first note that the terms in the right-hand-side of the x_f subsystem of Eq. (38) constitute an $O(\varepsilon)$ approximation to the term $\Lambda_{f\varepsilon}x_f$. Consider also the following linear system:

$$\varepsilon\frac{\mathrm{d}\bar{x}_f}{\mathrm{d}t} = \Lambda_{f\varepsilon}\bar{x}_f + \varepsilon\xi_f \tag{67}$$

which is exponentially stable. The exponential stability of the closed-loop infinite-dimensional system of Eq. (38) ensures that the zero solution of the x_f subsystem of Eq. (38) is exponentially stable, which guarantees that as $t \to \infty$, Cov_{hf} converges to a finite value. Now, we follow a similar approach to the one employed in the proof of Theorem A.1 in Kokotovic et al. (1986, p. 361) to compute the theoretical estimate of Cov_{hf}. Specifically, we have that there exists an $\hat{\varepsilon}^* > 0$ such that if $\varepsilon \in (0, \hat{\varepsilon}^*]$, we have that

$$x_f(t) = \bar{x}_f(t) + O(\sqrt{\varepsilon}) \tag{68}$$

Therefore, we have the following estimate for $\langle \|x_f(t)\|_2^2 \rangle$:

$$\langle \|x_f(t)\|_2^2 \rangle = \langle \|\bar{x}_f(t) + O(\sqrt{\varepsilon})\|_2^2 \rangle \leqslant 2\langle \|\bar{x}_f(t)\|_2^2 \rangle + O(\varepsilon) \tag{69}$$

where $\langle\cdot\rangle$ denotes the expected value and $\|\cdot\|_2$ is the standard Euclidean norm. Note that $\langle \|x_f(t)\|_2^2 \rangle$ and $\langle \|\bar{x}_f(t)\|_2^2 \rangle$ are equal to the traces of the covariance matrices of $x_f(t)$ and $\bar{x}_f(t)$, $P_f(t) = \langle x_f(t) x_f(t)^{\mathrm{T}} \rangle$ and $\bar{P}_f(t) = \langle \bar{x}_f(t) \bar{x}_f(t)^{\mathrm{T}} \rangle$, respectively. Finally, as $t \to \infty$, $P_f(t)$ and $\bar{P}_f(t)$ converge to P_f and $\bar{P}_f$, respectively (both P_f and $\bar{P}_f$ are bounded quantities which follows from closed-loop stability). Because $\Lambda_{f\varepsilon}$ is a stable diagonal matrix, the trace of matrix $\bar{P}_f$ can be computed as follows (Lou and Christofides, 2005a):

$$\mathrm{Tr}\{\bar{P}_f\} = \frac{\varepsilon}{2} \cdot \sum_{i=1}^{\infty} \left| \frac{1}{\lambda_{\varepsilon i}} \right| \tag{70}$$

where $\lambda_{\varepsilon i}$ $(i = 1, 2, \ldots, \infty)$ are the eigenvalues of the matrix $\Lambda_{f\varepsilon}$ in Eq. (67). Due to the structure of the eigenspectrum of the linear operator of Eq. (4), $\sum_{i=1}^{\infty} |1/\lambda_{\varepsilon i}|$ converges to a finite positive number, and thus, there exists a positive real number $k_{f\varepsilon}$ such that

$$\mathrm{Tr}\{\bar{P}_f\} < \frac{\varepsilon}{2} \cdot k_{f\varepsilon} \tag{71}$$

Therefore, it follows that

$$\mathrm{Tr}\{\bar{P}_f\} = \langle \|\bar{x}_f(\infty)\|_2^2 \rangle = O(\varepsilon) \tag{72}$$

According to Eq. (69), it follows that the contribution to the surface covariance from the state x_f of the infinite-dimensional system of Eq. (38) is $O(\varepsilon)$, i.e.,

$$\mathrm{Cov}_{hf} = \mathrm{Tr}\{P_f\} = \mathrm{Tr}\{\bar{P}_f\} + O(\varepsilon) = O(\varepsilon) + O(\varepsilon) = O(\varepsilon) \tag{73}$$

This completes the proof of Eq. (61). □

Proof of Eq. (63). We now focus on the x_s subsystem and the equation for the estimation error, e, in Eq. (38).

$$\begin{aligned} \frac{\mathrm{d}}{\mathrm{d}t}\begin{bmatrix} x_s \\ e \end{bmatrix} &= \begin{bmatrix} \Lambda_s + B_s G & -B_s G \\ \mathbf{0} & \Lambda_s - KC_s \end{bmatrix}\begin{bmatrix} x_s \\ e \end{bmatrix} + \begin{bmatrix} \mathbf{0} \\ -KC_f \end{bmatrix} x_f \\ &\quad + \begin{bmatrix} I_s & \mathbf{0} \\ I_s & -K \end{bmatrix}\begin{bmatrix} \xi_s \\ \xi_y \end{bmatrix} \end{aligned} \tag{74}$$

Let k_{1s} be a positive real number satisfying $k_{1s} > \|KC_f\|_2$ and we have the following:

$$\|KC_f x_f\|_2 < \|KC_f\|_2 \cdot \|x_f\|_2 < k_{1s}\|x_f\|_2 \tag{75}$$

From Eq. (68), we have the following estimate for $\|x_f\|_2$ for $t \geqslant t_b$ (where t_b is the time needed for $\|\bar{x}_f(t)\|_2$ to approach zero and $t_b \to 0$ as $\varepsilon \to 0$):

$$\|x_f(t)\|_2 = O(\sqrt{\varepsilon}) \tag{76}$$

This implies that we have the following estimate for $KC_f x_f(t)$ for $t \geqslant t_b$:

$$KC_f x_f(t) = O(\sqrt{\varepsilon}) \tag{77}$$

Furthermore, the exponential stability of the closed-loop infinite-dimensional system of Eq. (38) ensures that the zero solution of Eq. (74) is exponentially stable. Therefore, as $t \to \infty$, Cov_{hs} converges to a finite value. We now proceed to provide a theoretical estimate for Cov_{hs}. We first consider the equations for the estimation errors in both Eqs. (33) and (38). The estimation error of the finite-dimensional system of Eq. (33), $\tilde{e}$, is described by the following equation:

$$\frac{\mathrm{d}\tilde{e}}{\mathrm{d}t} = (\Lambda_s - KC_s)\tilde{e} + \xi_s - K\xi_y \tag{78}$$

The estimation error of the infinite-dimensional system of Eq. (38), e, is as follows:

$$\frac{\mathrm{d}e}{\mathrm{d}t} = (\Lambda_s - KC_s)e - KC_f x_f + \xi_s - K\xi_y \tag{79}$$

According to Eq. (77), the solution of Eq. (78) consists of an $O(\sqrt{\varepsilon})$ approximation of the solution of Eq. (79) (Kokotovic et al., 1986, Theorem A.1, p. 361). In particular, there exists an $\hat{\varepsilon}^{**} > 0$ such that for all $\varepsilon \in (0, \hat{\varepsilon}^{**}]$, it holds that

$$e(t) - \tilde{e}(t) = O(\sqrt{\varepsilon}) \tag{80}$$

Based on Eq. (80), the right-hand side of the $\tilde{x}_s$ system of Eq. (33) constitutes an $O(\sqrt{\varepsilon})$ approximation to the right-hand side of the x_s subsystem of Eq. (38). Therefore, the solution for $\tilde{x}_s$ of Eq. (33) consists of an $O(\sqrt{\varepsilon})$ approximation of the solution for the x_s of

Eq. (38) (Kokotovic et al., 1986, Theorem A.1, p. 361). In particular, there exists an $\hat{\varepsilon}^{***} > 0$ such that for all $\varepsilon \in (0, \hat{\varepsilon}^{***}]$, it holds that

$$x_s(t) - \tilde{x}_s(t) = O(\sqrt{\varepsilon}) \tag{81}$$

and

$$\begin{aligned} \|x_s(t)\|_2^2 - \|\tilde{x}_s(t)\|_2^2 &= (\|x_s(t)\|_2 - \|\tilde{x}_s(t)\|_2) \cdot (\|x_s(t)\|_2 + \|\tilde{x}_s(t)\|_2) \\ &= O(\sqrt{\varepsilon}) \end{aligned} \tag{82}$$

Because $\|x_s(t)\|_2$ and $\|\tilde{x}_s(t)\|_2$ are bounded for all $t > 0$, $\langle \|x_s(t)\|_2^2 \rangle$ and $\langle \|\tilde{x}_s(t)\|_2^2 \rangle$ are equal to the traces of the covariance matrices of $x_s(t)$ and $\tilde{x}_s(t)$, $P_s(t) = \langle x_s(t) x_s(t)^{\mathrm{T}} \rangle$ and $\tilde{P}_s(t) = \langle \tilde{x}_s(t) \tilde{x}_s(t)^{\mathrm{T}} \rangle$, respectively. Immediately, it follows that

$$\mathrm{Cov}_{hs} = \mathrm{Tr}\{P_s\} = \mathrm{Tr}\{\tilde{P}_s\} + O(\sqrt{\varepsilon}) = \widetilde{\mathrm{Cov}}_h + O(\sqrt{\varepsilon}) \tag{83}$$

This completes the proof of Eq. (63). □

Proof of Eq. (41) in Theorem 1. The surface covariance from the closed-loop infinite-dimensional system of Eq. (38), Cov_h, includes contributions from both x_s and x_f subsystems of Eq. (38). Therefore, we have the following equation for Cov_h:

$$\mathrm{Cov}_h = \mathrm{Cov}_{hs} + \mathrm{Cov}_{hf} \tag{84}$$

where Cov_{hf} and Cov_{hs} are defined in Eqs. (61)–(64). Using Eqs. (61) and (63), we immediately have

$$\mathrm{Cov}_h = \widetilde{\mathrm{Cov}}_h + O(\sqrt{\varepsilon}) + O(\varepsilon) \tag{85}$$

Since as $\varepsilon \to 0$, it holds that

$$\frac{O(\varepsilon)}{O(\sqrt{\varepsilon})} \to 0 \tag{86}$$

Therefore, the $O(\varepsilon)$ term in Eq. (85) is very small relative to the term $O(\sqrt{\varepsilon})$ and can be neglected. There exists an $\varepsilon^* = \min(\hat{\varepsilon}, \hat{\varepsilon}^*, \hat{\varepsilon}^{**}, \hat{\varepsilon}^{***})$ such that if $\varepsilon \in (0, \varepsilon^*]$, then

$$\mathrm{Cov}_h = \widetilde{\mathrm{Cov}}_h + O(\sqrt{\varepsilon}) \tag{87}$$

This completes the proof of Theorem 1. □

References

Akiyama, Y., Imaishi, N., Shin, Y.S., Jung, S.C., 2002. Macro- and micro-scale simulation of growth rate and composition in MOCVD of yttria-stabilized ziroconia. Journal of Crystal Growth 241, 352–362.

Armaou, A., Siettos, C.I., Kevrekidis, I.G., 2004. Time-steppers and 'coarse' control of distributed microscopic processes. International Journal of Robust and Nonlinear Control 14, 89–111.

Åström, K.J., 1970. Introduction to Stochastic Control Theory. Academic Press, New York.

Baker, J., Christofides, P.D., 1999. Output feedback control of parabolic PDE systems with nonlinear spatial differential operators. Industrial & Engineering Chemistry Research 38, 4372–4380.

Ballestad, A., Ruck, B.J., Schmid, J.H., Adamcyk, M., Nodwell, E., Nicoll, C., Tiedje, T., 2002. Surface morphology of gas during molecular beam epitaxy growth: comparison of experimental data with simulations based on continuum growth equations. Physical Review B 65, 205302.

Bohlin, T., Graebe, S.F., 1995. Issues in nonlinear stochastic grey-box identification. International Journal of Adaptive Control and Signal Processing 9, 465–490.

Choo, J.O., Adomaitis, R.A., Henn-Lecordier, L., Cai, Y., Rubloff, G.W., 2005. Development of a spatially controllable chemical vapor deposition reactor with combinatorial processing capabilities. Review of Scientific Instruments 76, 062217.

Christofides, P.D., 2001. Nonlinear and Robust Control of PDE Systems: Methods and Applications to Transport-Reaction Processes. Birkhäuser, Boston.

Christofides, P.D., Armaou, A., 2006. Control and optimization of multiscale process systems. Computers & Chemical Engineering 30, 1670–1686.

Christofides, P.D., Baker, J., 1999. Robust output feedback control of quasi-linear parabolic PDE systems. Systems & Control Letters 36, 307–316.

Christofides, P.D., Daoutidis, P., 1997. Finite-dimensional control of parabolic PDE systems using approximate inertial manifolds. Journal of Mathematical Analysis and Applications 216, 398–420.

Christofides, P.D., Armaou, A., Lou, Y., Varshney, A., 2008. Control and Optimization of Multiscale Process Systems. Birkhäuser, Boston (accepted for publication).

Cuerno, R., Makse, H.A., Tomassone, S., Harrington, S.T., Stanley, H.E., 1995. Stochastic model for surface erosion via ion sputtering: dynamical evolution from ripple morphology to rough morphology. Physical Review Letters 75, 4464–4467.

Edwards, S.F., Wilkinson, D.R., 1982. The surface statistics of a granular aggregate. Proceedings of the Royal Society of London, Series A: Mathematical Physical and Engineering Sciences 381, 17–31.

Gallivan, M.A., Murray, R.M., 2004. Reduction and identification methods for Markovian control systems, with application to thin film deposition. International Journal of Robust and Nonlinear Control 14, 113–132.

Hotz, A., Skelton, R.E., 1987. Covariance control theory. International Journal of Control 46, 13–32.

Hu, G., Lou, Y., Christofides, P.D., 2008. Model parameter estimation and feedback control of surface roughness in a sputtering process. Chemical Engineering Science 63, 1800–1816.

Insepov, Z., Yamada, I., Sosnowski, M., 1997. Surface smoothing with energetic cluster beams. Journal of Vacuum Science & Technology A—Vacuum Surfaces and Films 15, 981–984.

Iwasaki, T., Skelton, R.E., 1994. On the observer-based structure of covariance controllers. Systems & Control Letters 22, 17–25.

Kan, H.C., Shah, S., Tadyyon-Eslami, T., Phaneuf, R.J., 2004. Transient evolution of surface roughness on patterned GaAs(0 0 1) during homoepitaxial growth. Physical Review Letters 92, 146101.

Kardar, M., Parisi, G., Zhang, Y.C., 1986. Dynamic scaling of growing interfaces. Physical Review Letters 56, 889–892.

Kokotovic, P.V., Khalil, H.K., O'Reilly, J., 1986. Singular Perturbations in Control: Analysis and Design. Academic Press, London.

Kristensen, N.R., Madsen, H., Jorgensen, S.B., 2004. Parameter estimation in stochastic grey-box models. Automatica 40, 225–237.

Lauritsen, K.B., Cuerno, R., Makse, H.A., 1996. Noisy Kuramote–Sivashinsky equation for an erosion model. Physical Review E 54, 3577–3580.

Lee, Y.H., Kim, Y.S., Ju, B.K., Oh, M.H., 1999. Roughness of ZnS: Pr, Ce/Ta_2O_5 interface and its effects on electrical performance of alternating current thin-film electroluminescent devices. IEEE Transactions on Electron Devices 46, 892–896.

Lou, Y., Christofides, P.D., 2003a. Estimation and control of surface roughness in thin film growth using kinetic Monte-Carlo models. Chemical Engineering Science 58, 3115–3129.

Lou, Y., Christofides, P.D., 2003b. Feedback control of growth rate and surface roughness in thin film growth. A.I.Ch.E. Journal 49, 2099–2113.

Lou, Y., Christofides, P.D., 2004. Feedback control of surface roughness of GaAs (0 0 1) thin films using kinetic Monte-Carlo models. Computers & Chemical Engineering 29, 225–241.

Lou, Y., Christofides, P.D., 2005a. Feedback control of surface roughness in sputtering processes using the stochastic Kuramoto–Sivashinsky equation. Computers & Chemical Engineering 29, 741–759.

Lou, Y., Christofides, P.D., 2005b. Feedback control of surface roughness using stochastic PDEs. A.I.Ch.E. Journal 51, 345–352.

Lou, Y., Christofides, P.D., 2006. Nonlinear feedback control of surface roughness using a stochastic PDE: design and application to a sputtering process. Industrial & Engineering Chemistry Research 45, 7177–7189.

Ni, D., Christofides, P.D., 2005a. Dynamics and control of thin film surface microstructure in a complex deposition process. Chemical Engineering Science 60, 1603–1617.

Ni, D., Christofides, P.D., 2005b. Multivariable predictive control of thin film deposition using a stochastic PDE model. Industrial & Engineering Chemistry Research 44, 2416–2427.

Qi, H.J., Huang, L.H., Tang, Z.S., Cheng, C.F., Shao, J.D., Fan, Z.X., 2003. Roughness evolution of ZrO_2 thin films grown by reactive ion beam sputtering. Thin Solid Films 444, 146–152.

Rusli, E., Drews, T.O., Ma, D.L., Alkire, R.C., Braatz, R.D., 2006. Robust nonlinear feedforward-feedback control of a coupled kinetic Monte Carlo-finite difference simulation. Journal of Process Control 16, 409–417.

Siettos, C.I., Armaou, A., Makeev, A.G., Kevrekidis, I.G., 2003. Microscopic/stochastic timesteppers and "coarse" control: a kMC example. A.I.Ch.E. Journal 49, 1922–1926.

Theodoropoulou, A., Adomaitis, R.A., Zafiriou, E., 1998. Model reduction for optimization of rapid thermal chemical vapor deposition systems. IEEE Transactions on Semiconductor Manufacturing 11, 85–98.

Varshney, A., Armaou, A., 2005. Multiscale optimization using hybrid PDE/kMC process systems with application to thin film growth. Chemical Engineering Science 60, 6780–6794.

Varshney, A., Armaou, A., 2006. Identification of macroscopic variables for low-order modeling of thin-film growth. Industrial & Engineering Chemistry Research 45, 8290–8298.

Villain, J., 1991. Continuum models of crystal growth from atomic beams with and without desorption. Journal de physique I 1, 19–42.

Vvedensky, D.D., Zangwill, A., Luse, C.N., Wilby, M.R., 1993. Stochastic equations of motion for epitaxial growth. Physical Review E 48, 852–862.